journal

J. Am. Ceram. Soc., **80** [12] 3193–98 (1997)

Formation and Structural Characterization of 1:1 Ordered Perovskites in the $Ba(Zn_{1/3}Ta_{2/3})O_3$–$BaZrO_3$ System

Liang Chai* and Peter K. Davies*

Department of Materials Science and Engineering, University of Pennsylvania, Philadelphia, Pennsylvania 19104-6272

The phase stabilities in the $(1-x)Ba(Zn_{1/3}Ta_{2/3})O_3$ (BZT)–$xBaZrO_3$ (BZ) system have been investigated using samples prepared by the mixed-oxide method. The substitution of Zr^{4+} destabilizes the 1:2 cation ordering in BZT and promotes the formation of a cubic, 1:1 ordered structure with a doubled perovskite repeat. The homogeneity range of the 1:1 phase extends from $x = 0.04$ to approximately $x = 0.25$; substitutions beyond this range stabilize a disordered perovskite. The limits of stability of the 1:1 ordering coincide with compositions previously found to exhibit anomalies in their dielectric loss. The range of homogeneity is consistent with a ''random layer'' model for the 1:1 ordered ''$Ba\{\beta'_{1/2}\beta''_{1/2}\}O_3$'' structure. In this model the β'' positions are assumed to be occupied exclusively by Ta^{5+}, and the β' sites by a random distribution of Zn^{2+}, Zr^{4+}, and the remaining Ta^{5+} cations. The validity of the model, where the ordered solid solutions can be represented by $Ba\{[Zn_{(2-y)/3}Ta_{(1-2y)/3}Zr_y]_{1/2}[Ta]_{1/2}\}O_3$ ($y = 2x$) was confirmed by Rietveld refinements conducted using data collected with a synchrotron X-ray source.

I. Introduction

THE very low dielectric losses of perovskite ceramics based on $Ba(Zn_{1/3}Ta_{2/3})O_3$ (BZT) have led to their widespread application as filters and oscillators in wireless communication devices.[1–6] In the most stable form of BZT the Zn^{2+} and Ta^{5+} cations order onto individual (111) planes of the perovskite subcell (see Fig. 1(a)). The long-range ordering and associated displacement of the oxygen anions between the cation planes yield a trigonal supercell (space group $P\bar{3}m1$) with a ''1:2'' {ZnTaTa} layer repeat.[7,8] In BZT, and also in the related $Ba(Mg_{1/3}Ta_{2/3})O_3$ (BMT) system, the formation of a defect-free, fully ordered cation arrangement is critical in optimizing the dielectric response. In previous papers[5,9] we have discussed the relationship between the loss properties and cation correlations in BZT in terms of the nucleation and growth of different orientational variants of the 1:2 structure. Short-term annealed ceramics are comprised of small domains of each ordered variant and have low Q (<1000) values. The growth of the domains and associated reduction in the volume of high-loss domain boundaries were suggested as being responsible for the very large improvement in Q (>12000 at 10 GHz) after extended thermal treatment.

The long anneal times required to access high Q values in pure BZT have led to the development of alternate, more cost-effective methods for stabilizing a low-loss state with a short sintering time. Tamura *et al.*[2] first showed that this could be achieved through the substitution of small concentrations of $BaZrO_3$ (BZ). Additions up to ~4 mol% BZ reduce the time required to access a high Q state to ≤10 h at ~1500°C. Recent studies[5,9] using HRTEM have shown that samples with ≤~3 mol% BZ retain the 1:2 structure of BZT, but are comprised of ordered domains whose size decreases as the Zr concentration is increased. The reduction in the length scale of the cation correlations was found to parallel the decrease in the annealing time required to access a low-loss state. Although any reduction in the size of the ordered domains in pure BZT decreases Q, in the BZ-substituted ceramics a high Q is maintained even though they contain a very high volume of domain boundaries. We proposed that the stabilization and lowering of the losses at the boundaries was due to the partial segregation of the Zr cations.

Tamura *et al.*[2] also reported that the Q values in the BZT–BZ system increased to 15 000 with additions up to approximately 4 mol% BZ, decreased to 10 000 at 25 mol%, and then rapidly deteriorated at higher level substitutions. HRTEM investigations[5,9] revealed that compositions close to the first anomaly in Q undergo a phase transformation to a structure comprised of cubic 1:1 ordered nanodomains with a doubled perovskite repeat. The cation ordering in the 1:1 ''$Ba\{\beta'_{1/2}\beta''_{1/2}\}O_3$'' phase was interpreted using a ''random layer'' structure model. In this structure the β'' sites were assumed to be occupied exclusively by Ta, and the β' positions by a random mixture of Zn^{2+}, Zr^{4+}, and the remaining Ta^{5+} cations (see Fig. 1(b)).

In this paper we extend our studies of the BZT–BZ system to compositions beyond 5 mol% BZ, and explore the phase stabilities across the entire pseudobinary. We also report on refinements of the crystal structures of the 1:1 ordered phases using Rietveld techniques. The results of these investigations are related to the dielectric properties of the BZT–BZ solid solutions.

II. Experimental Procedures

(1) Sample Preparation and Characterization

Samples in the $(1-x)Ba(Zn_{1/3}Ta_{2/3})O_3$–$xBaZrO_3$ solid solution system were prepared with $x = 0.075$, 0.15, 0.25, 0.35, 0.4, and 0.5 from predried, high-purity (≥99.9%) commercial powders of $BaCO_3$, ZnO, Ta_2O_5, and ZrO_2. After weighing, the stoichiometric mixtures were first heated in air at 1100°C to remove CO_2, and then reground and calcined at 1300°C for 10 h. After a second regrinding, the powders were pressed and sintered at 1425°C. The achievement of an equilibrium state was gauged by the absence of any changes in the X-ray patterns after an additional heat treatment at 1425°C. In general, the low-temperature pretreatments were found to be effective in inhibiting the loss of Zn at higher temperatures. However, as an additional precaution samples of the higher Zn contents were buried in a powder with the same stoichiometry and covered with an inverted platinum crucible. Phase identification was

R. S. Roth—contributing editor

Manuscript No. 191214. Received February 11, 1997; approved April 24, 1997.

This work was supported by the National Science Foundation (DMR94-21184). The facilities at the National Synchrotron Light Source, Brookhaven National Laboratory, are supported by the U.S. Department of Energy, Division of Materials Sciences and Division of Chemical Sciences. We also acknowledge the support of the electron microscopy facilities by the National Science Foundation MRSEC program, award No. DMR-96-32598.

*Member, American Ceramic Society.

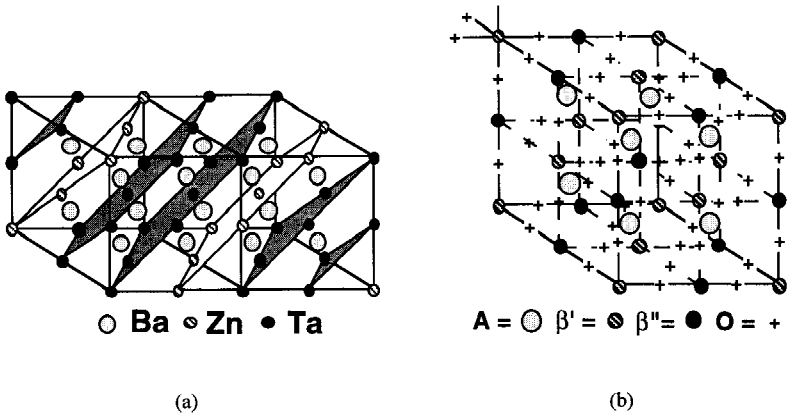

Fig. 1. Schematic illustrations of (a) the 1:2 ordering of Zn and Ta in $Ba(Zn_{1/3}Ta_{2/3})O_3$, oxygen omitted for clarity; (b) the cubic, $Fm\bar{3}m$ doubled perovskite cell of the 1:1 ordered $A(\beta'_{1/2}\beta''_{1/2})O_3$ structure.

conducted using a Rigaku DMAX-B X-ray diffractometer with a conventional Cu*K*α source. Lattice parameters were calculated by least-squares refinement of data collected with an internal Si standard.

(2) Synchrotron Data Collection

Synchrotron X-ray data for samples with $x = 0.15$ and 0.25 were collected on the X7A beamline at the National Synchrotron Light Source, Brookhaven National Laboratory. A Ge(111) crystal was used as a monochromator for the incident beam, and the wavelength (0.6989 Å) was calibrated using a silicon standard. Data were collected on a horizontally mounted, flat-plate sample using a 0.5 mm × 14 mm receiving slit. The sampling intervals were 0.01° (2θ) for $x = 0.15$ and 0.016° (2θ) for $x = 0.25$. The final integrated intensities were calculated by comparing the counts from the diffracted beam to those of the incident beam, and were scaled to 100 mA beam current to account for any variation during the experiment.

(3) Rietveld Refinement

All of the peaks in the synchrotron X-ray diffraction patterns could be indexed using a face-centered-cubic cell ($Fm\bar{3}m$) with a doubled perovskite repeat. In this supercell the β′ and β″ positions in the $Ba\{\beta'_{1/2}\beta''_{1/2}\}O_3$ structure adopt a NaCl type of arrangement. Reflections arising from the cation ordering have indices all odd, while reflections with (*hkl*) all even arise from the scattering of the perovskite subcell. The reflections from the superstructure in the patterns of both samples were broader than those from the subcell. The peak broadening was consistent with the formation of domain structures that have been observed previously in this system and also in other related mixed-metal perovskites.[9,10] To obtain an adequate fit to all of the reflections it was necessary to conduct the Rietveld refinements using two sets of peak fitting parameters, one for the supercell and one for the subcell. This procedure has been used previously in the refinement of domain-limited ordered structures in $A_2(M^{3+}M^{5+})O_6$ perovskites.[10] To fit the two sets of peaks, a UNIX version of the Rietveld program RIETAN was used for the refinements of the synchrotron X-ray data.[10,11] The peak profiles were modeled using a five-parameter modified pseudo-Voigt function. The coefficients for the real and imaginary components of dispersion corrections (f' and f'') for all ions were calculated using the subroutine in the GSAS program package.[12]

The random layer structure model (see Section III) was used as a starting point for the refinements. The scale factors, zero correction, background coefficients, unit-cell parameters, two sets of peak profile parameters, oxygen position, cation occupancies, and isotropic temperature parameters were all refined. All of the cation sites were assumed to be fully occupied, and the total concentration of each cation was constrained to the overall chemical composition. Multiple cations occupying a given site were assumed to have the same isotropic thermal parameter. Williamson–Hall plots were used to characterize the size and strain within the ordered domains.[10,13,14]

III. Results

(1) Phase Stabilities

The $(1 - x)$BZT–xBZ solid solutions were found to adopt an equilibrium phase assemblage, gauged by the lack of any change in the X-ray patterns after a repeat firing, after two or three heat treatments at 1425°C (see Table I). In general, the precautions that were used to inhibit the loss of zinc were successful in avoiding any competing decomposition reactions. Weak additional reflections that could be ascribed to ''non-equilibrium'' phases were only observed in samples with $x = 0.075$ that had been heated for longer than 25 h. The final X-ray patterns collected from the solid solutions with $x = 0.075$–0.5 are presented in Fig. 2. This figure also includes data from samples with $x = 0.01$, 0.02, and 0.04 that had been collected in the previous study of Davies *et al.*[9] From this figure it is evident that the substitution of BZ into BZT induces several changes in the intensities and positions of the reflections associated with the ordering of the B-site cations. For 1% substitution the strong and sharp supercell reflections originate from the trigonal 1:2 ordered structure. These reflections broaden and weaken as the substitution level is raised to $x = 0.02$, and disappear in the samples with $x = 0.04$. For $x = 0.075$ a new set of superstructure reflections appear at positions that correspond to the formation of a face-centered-cubic, 1:1 ordered supercell with $a = 2a_{subcell}$. These new reflections become sharper and stronger in samples with $x = 0.15$ and 0.25. For $x = 0.35$ the *X*-ray patterns still show evidence for the formation of the doubled cubic cell, though the reflections are very weak and diffuse. Samples with a higher Zr content, e.g., $x =$

Table I. Unit-Cell Parameters and Preparation Conditions for $(1 - x)Ba(Zn_{1/3}Ta_{2/3})O_3 - xBaZrO_3$

x	a (Å)	c (Å)	Subcell volume (Å^3)	Sintering time (h)
0.0†	5.780 (1)	7.104 (1)	68.51	
0.075	8.2070 (7)		69.10	35
0.15	8.2194 (19)		69.41	30
0.25	8.2442 (12)		70.04	25
0.35	4.1302 (6)		70.46	25
0.40	4.1379 (9)		70.85	35
0.50	4.1439 (7)		71.16	20
1.0‡	4.193		73.72	

†From Ref 7. ‡From JCPDF Diffraction File No. 6-399.

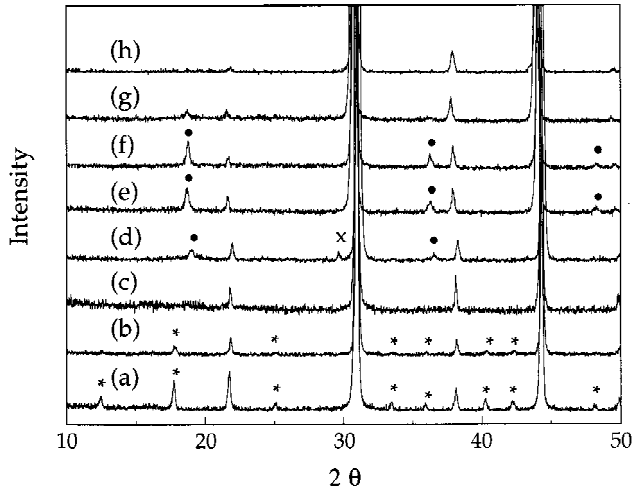

Fig. 2. X-ray diffraction patterns for $(1 - x)$BZT–xBZ solid solutions with x = (a) 0.01, (b) 0.02, (c) 0.04, (d) 0.075, (e) 0.15, (f) 0.25, (g) 0.35, (h) 0.5. Supercell reflections from 1:2 order indicated by *, from 1:1 order by solid circles. Minor impurity in $x = 0.075$ labeled by X. Patterns (a), (b), and (c) are taken from Ref. 9.

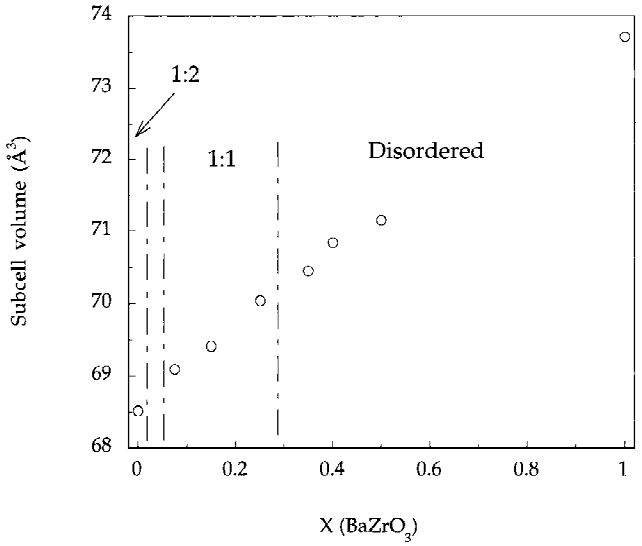

Fig. 4. Variation of the volume of the perovskite subcell with composition in the $(1 - x)$BZT–xBZ system. Vertical dashed lines show approximate locations of boundaries separating the 1:2, 1:1, and disordered perovskite phase fields.

0.4 or 0.5, show no evidence for any cation ordering and can be indexed using a disordered, $Pm\bar{3}m$, perovskite cell.

Further information on the changes in the cation ordering was obtained from the $x = 0.04$ sample using data collected with a synchrotron X-ray source (normalized to $\lambda = 0.6989$ Å). Although the scan of this sample in Fig. 2, which utilized a conventional X-ray tube, does not show any evidence for cation order, the pattern obtained using synchrotron X-rays (Fig. 3) contains very broad supercell reflections. These reflections are centered at positions that can be indexed using the face-centered cubic cell with $a = 2a_{\text{subcell}}$. Figure 3 shows the broad (111) reflection of the supercell in the lower angle region of the scan. The size of the ordered domains, calculated using the Scherrer formula, that give rise to this reflection is approximately 30 Å. This value is consistent with previous HRTEM studies of this sample in which the structure was found to be comprised of 20–45 Å, 1:1 ordered domains.

The X-ray studies indicate that the ordered 1:2 structure of BZT has a very narrow range of stability in the BZT–BZ system. The transformation to a ''1:1'' ordered structure at $x = 0.04$ is consistent with the previous TEM results, which also showed evidence for a very narrow two-phase region in samples with $x = 0.03$. In contrast, the patterns in Figs. 2 and 3 reveal that the 1:1 ordered structure has a broad range of homogeneity that extends from $x = 0.04$ to approximately $x = 0.25$. The transition to a fully disordered perovskite begins at substitution levels beyond 25 mol% BZ, though it is unclear from these results whether this is a continuous or a first-order transition. A complete listing of the cell parameters across the system is given in Table I together with the volume of the perovskite subcell at each composition. As expected from the relative differences in the ionic radii of the B-site cations (0.72 Å for Zr^{4+}; and 0.675 Å for $\frac{1}{3}(Zn^{2+}) + \frac{2}{3}(Ta^{5+})$), the cell volumes increase with increasing BZ. However, the variation in volume with composition is not linear and small discontinuities are apparent in the vicinity of the phase boundaries (see Fig. 4).

(2) 1:1 Order:Structure Refinement

The formation of a face-centered-cubic 1:1 ordered superstructure is commonly observed in $A(B'_{1/2}B''_{1/2})O_3$ mixed-metal

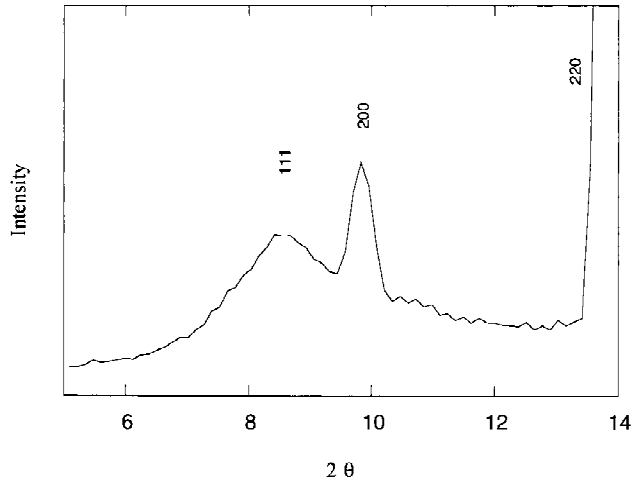

Fig. 3. Low-angle region of a pattern of $x = 0.04$ collected using synchrotron X-rays. Indexing is in terms of a doubled cubic supercell.

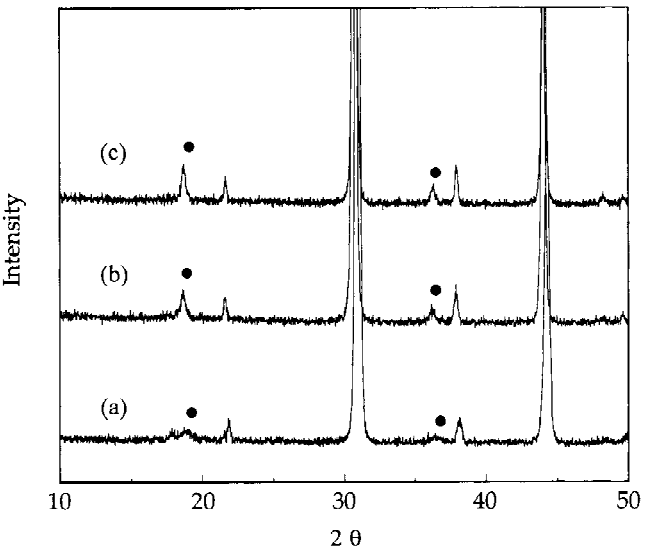

Fig. 5. X-ray patterns collected from $x = 0.15$ after heating at 1425°C for (a) 10, (b) 20, (c) 30 h. 1:1 ordering reflections indicated by filled circles.

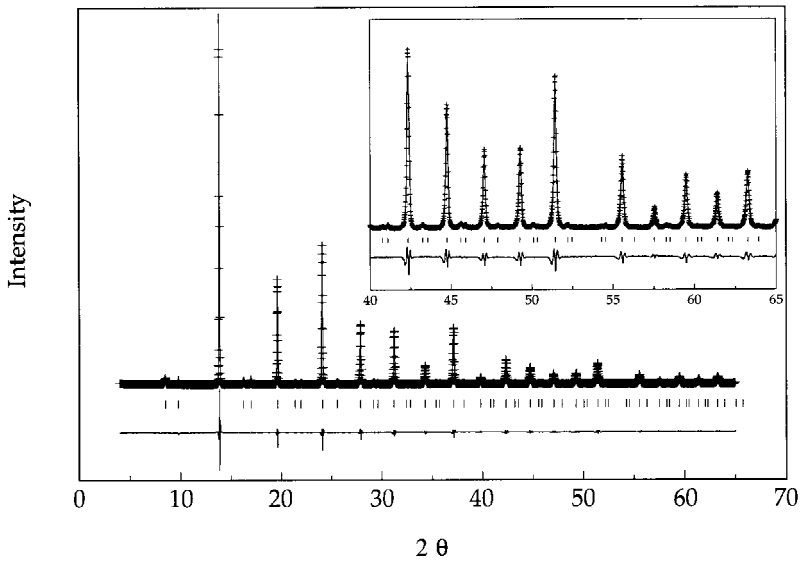

Fig. 6. Experimental, calculated, and difference profiles for $x = 0.15$. Inset shows enlargement of higher angle region.

perovskites when the octahedral sites contain a 1:1 distribution of two different cations.[7] For those systems the doubled cell edge arises from an ordered alternation of the B′ and B″ cations on the β′ and β″ sites of the $A(\beta'_{1/2}\beta''_{1/2})O_3$ structure (see Fig. 1(b)). The stability of this superstructure is derived from the minimization of the cation–cation coulombic repulsions, each B′ ion has six B″ neighbors, and from the accommodation of differences in the B′–O and B″–O bond lengths via the displacement of the oxygen anions. Although most 1:2 $A(B'_{1/3}B''_{2/3})O_3$ perovskites adopt a trigonal 1:2 superstructure, 1:1 chemical ordering is observed in $Pb(M^{2+}_{1/3}M^{5+}_{2/3})O_3$ relaxor ferroelectrics[15–17] (M^{2+} = Mg, Ni, Zn, etc.; M^{5+} = Nb, Ta) and hexavalent $A(M^{6+}_{1/3}M^{3+}_{2/3})O_3$ systems (A = Ba, Sr; M^{3+} = Al, Fe, Sc, rare earth; M^{6+} = W, U, Re).[7,18–21] For the $Pb(M^{2+}_{1/3}M^{5+}_{2/3})O_3$ relaxors the ordering, which is limited to small nanosized domains, has been interpreted through the ''space-charge'' model.[15,17,22] In this model it is claimed that the β′ and β″ positions are occupied exclusively by the M^{2+} and M^{5+} cations and that the resultant charge imbalance is compensated by a M^{5+}-rich disordered matrix that surrounds the domains. Support for the two-phase space charge model has come from the absence of any domain growth with extended annealing.[17,22]

Because the 1:1 phases in the BZT–BZ solid solutions are stabilized by the incorporation of Zr on the octahedral sites, it is difficult to rationalize the ordering in this system in terms of a space-charge type model with a 1:1 distribution of Zn and Ta on the β′ and β″ positions. If this was the case, a 1:1 ordered superstructure would also be expected for the BZT end-member. The formation of a two-phase ''nanodomain + disordered matrix'' assemblage would also produce a splitting or broadening of the reflections from the perovskite subcell. There was no evidence for any type of subcell peak broadening in the patterns collected from the samples with $0.04 < x < 0.25$ that lie in the region of stability of the 1:1 phase. Studies of the evolution of the ordering also showed that the supercell peaks sharpen and strengthen with the anneal time, and provide evidence for the growth of the ordered domains (see Fig. 5). Moreover, TEM studies made on samples in the closely related $Ba(Mg_{1/3}Ta_{2/3})O_3$–$BaZrO_3$ system,[23] in which the phase relations are essentially identical to those in BZT–BZ, found no evidence for the existence of significant fractions of a disordered matrix in the 1:1 ordered compositions. For these reasons the structure refinements of the 1:1 BZT–BZ phases were conducted using a random layer model for the chemical order.

Although a random layer model for the 1:1 ordering of 1:2 perovskites has been suggested previously,[24–26] it has not found widespread support. In this model the β′ sites in the 1:1 $A(\beta'_{1/2}\beta''_{1/2})O_3$ phases are assumed to contain a random distribution of the M^{2+} and M^{5+} cations in a 2:1 ratio, the β″ positions are occupied exclusively by M^{5+}, and the structural formula of a 1:2 perovskite can be represented as $A\{[B^{2+}_{2/3}\text{-}B^{5+}_{1/3}]_{1/2}[B^{5+}]_{1/2}\}O_3$. Extending this model to the BZT–BZ system we have proposed that the β″ positions are still populated by Ta, but that the β′ sites now contain a random distribution of Zr, Zn, and the remaining Ta cations. The formula of this form of the 1:1 ordered $(1 - x)$BZT–xBZ solid solutions can be represented as $Ba\{[Zn_{(2-y)/3}Ta_{(1-2y)/3}Zr_y]_{1/2}[Ta]_{1/2}\}O_3$, where $y = 2x$. Because the concentration of Zn:Ta in the random layer of a 1:1 BZT end-member would be 2:1, but their replacement by Zr is in a 1:2 ratio (yZr = (y/3)Zn + (2y/3)Ta), it is apparent that the random layer model could be valid for compositions up to 25 mol% BZ. This range of homogeneity is consistent with the experimentally observed limits described above.

To provide direct support for the model, diffraction data for samples with $x = 0.15$ and 0.25 were collected using synchrotron X-rays and refined using the Rietveld method. All of the peaks observed in the synchrotron X-ray diffraction patterns (Fig. 6) could be indexed using an $Fm\bar{3}m$ space group and a doubled perovskite cell, $a = 2a_{\text{subcell}}$. With this more intense

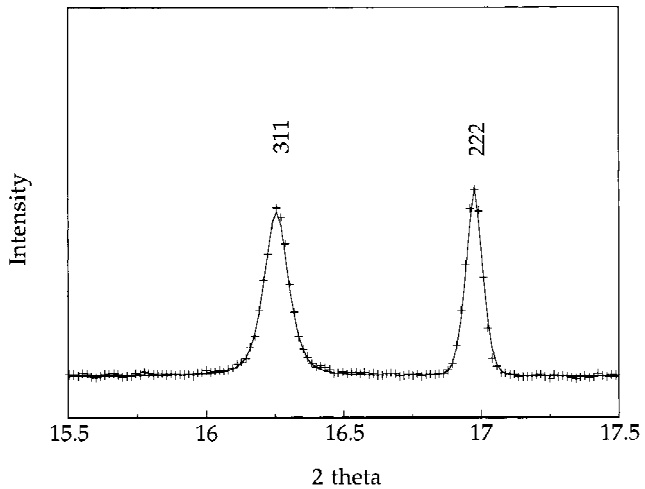

Fig. 7. Profile fits (solid lines) to experimental data (crosses) for the supercell (311) and subcell (222) reflections in $x = 0.25$.

Table II. Refined Structure Data for $x = 0.15$†

Atom	x	y	z	B_{iso} (Å^2)	Occupancy	
					Refined	"Random layer"
Ta (β')	0.0	0.0	0.0	0.28	0.249	0.133
Zn (β')	0.0	0.0	0.0	0.28	0.457	0.567
Zr (β')	0.0	0.0	0.0	0.28	0.294	0.300
Ta (β")	0.5	0.5	0.5	0.28	0.884	1.0
Zn (β")	0.5	0.5	0.5	0.28	0.110	0.0
Zr (β")	0.5	0.5	0.5	0.28	0.006	0.0
Ba	0.25	0.25	0.25	0.63	1.0	1.0
O	0.257	0.0	0.0	0.57	1.0	1.0

†Space group $Fm\bar{3}m$, $a = 8.2222$ Å.

Table III. Refined Structure Data for $x = 0.25$

Atom	x	y	z	B_{iso} (Å^2)	Occupancy	
					Refined	"Random layer"
Ta (β')	0.0	0.0	0.0	0.21	0.162	0.0
Zn (β')	0.0	0.0	0.0	0.21	0.346	0.50
Zr (β')	0.0	0.0	0.0	0.21	0.492	0.50
Ta (β")	0.5	0.5	0.5	0.21	0.838	1.0
Zn (β")	0.5	0.5	0.5	0.21	0.154	0.0
Zr (β")	0.5	0.5	0.5	0.21	0.008	0.0
Ba	0.25	0.25	0.25	0.61	1.0	1.0
O	0.256	0.0	0.0	0.27	1.0	1.0

†Space group $Fm\bar{3}m$, $a = 8.2478$ Å.

X-ray source many of the weaker high-angle reflections, which could not be detected by standard X-rays, were easily observed. Because the reflections originating from the supercell were somewhat broader than those from the perovskite subcell, the patterns were modeled using two sets of independent peak fitting parameters (see Experimental Section) which permitted an excellent fit to the observed profiles (see Fig. 7). Final reliability factors $R_{wp} = 0.11$, R_F(sub) $= 0.018$, R_F(super) $= 0.023$, and $R_{wp} = 0.088$, R_F(sub) $= 0.012$, R_F(super) $= 0.020$ were obtained for $x = 0.15$ and 0.25, respectively. The refined cell parameters, which were in close agreement with those determined in the phase stability studies, final atomic positions, and site occupancies for both samples are provided in Tables II and III. The validity of the final refined occupancies and bond lengths was supported by calculations of the site valences using the bond valence method.[27,28] Given the multiple occupancies of the cation sites, the calculated valence sums of all the positions are in very good agreement with those expected from the formal charges (see Table IV).

The occupancy of the β′ and β″ sites is compared to that predicted by a random layer model with $Ba\{[Zn_{(2-y)/3}Ta_{(1-2y)/3}Zr_y]_{1/2}[Ta]_{1/2}\}O_3$ in Tables II and III. For both samples the agreement between the experimental and predicted occupancies is good. There is very clear evidence for the concentration of Ta (>83%) in the β″ sites and for the occupation of the β′ sites by Zn, Zr, and Ta. While the small differences in the predicted and experimental occupancies suggest that the structure shows some degree of antisite disorder, it should be noted that both samples are comprised of ordered domains, which from Williamson–Hall plots were estimated to be 307 Å for $x = 0.15$ and 418 Å for $x = 0.25$. Therefore, the refined occupancies also contain contributions from the locally disordered anti-phase boundaries that separate the different translational variants of the 1:1 structure.

Table IV. Bond Distances and Site Valences

Site	M–O distance (Å)	Site valence	
		Calculated	Formal charge
$x = 0.15$			
Ba	2.908 (1)	2.26	2.00
β'	2.117 (1)	2.86	3.34
β"	1.995 (1)	4.66	4.66
O		−2.01	−2.00
$x = 0.25$			
Ba	2.916 (1)	2.21	2.00
β'	2.107 (1)	3.14	3.47
β"	2.016 (1)	4.32	4.53
O		−1.98	−2.00

IV. Discussion and Conclusions

The results of this investigation of the $(1 - x)$BZT–xBZ system show that very small concentrations of Zr ($x = 0.04$) promote a transformation to a 1:1 cation ordered state. The 1:1 phase is stable over a relatively broad range of homogeneity, $0.04 \leq x < \sim 0.25$, and its structure can be successfully interpreted using a random layer model. The effectiveness of a tetravalent substituent in promoting this type of transformation in a 1:2 mixed-metal perovskite has not been reported previously. The destabilization of the 1:2 ordered form of BZT by such low levels of BZ implies that the Zr^{4+} cations frustrate the longer-range interactions that are responsible for its stability. In particular we feel the mismatch in the Ta–O and Zr–O bond lengths inhibits the displacements of the oxygen anion layers which are a critical feature of the trigonal 1:2 ordered BZT structure. While it is perhaps clear why the random substitution of Zr onto the Zn and Ta layers would increase the free energy of 1:2 ordered BZT, it is not as obvious why the 1:1 ordered random layer structure is a stable alternative. In a previous publication we speculated that the formation of the random layer structure is an ''energetic compromise'' in which the ordering of Ta on one site (β″) is preserved at the expense of the others.[9] The stability of the 1:1 phase is partially derived from the ordering of the Ta cations on the β″ sites, which permits the correlated approach of the nearest-neighbor anions and the formation of an equilibrium Ta–O bond. Although no favorable contributions to the enthalpic stability will result from the ion distributions on the β′ positions, which contain a random mixture of Zn, Zr, and Ta, they do provide a significant favorable entropic contribution to the free energy. According to the idealized random layer model for the 1:1 ordered phases, which gives good agreement with the structure refinements, the composition of the β′ positions is given by $Zn_{(2-y)/3}Ta_{(1-2y)/3}Zr_y$ where $y = 2x$. In this model it is possible

to incorporate all of the Zr cations into the random layer up to 25 mol% BZ substitution ($y = 0.5$), which is in excellent agreement with the observed range of homogeneity. Substitution beyond this level would require the incorporation of Zr onto the β (Ta) positions which, given the arguments presented above for the destabilization of the 1:2 structure, would be expected to produce a large reduction in the overall stability. This conclusion is supported by the observation of a transition to a disordered perovskite at higher values of *x*. Using an ideal solution model for the mixing on the β′ sites, the gain in configurational entropy for 1 mol of β′ positions, i.e., for 2 mol of the $Ba(\beta'_{1/2}\beta''_{1/2})O_3$ phases, is given by

$$\Delta S = (-R\{[(2-y)/3]\ln[(2-y)/3] + [(1-2y)/3]\ln[(1-2y)/3] + y\ln y\}$$

The entropy derived from the β′ site mixing is significant across the entire range of y ($0 \leq y \leq 0.5$) with a maximum at 0.25 (i.e., 12.5 mol% BZ). This contribution is apparently sufficient to offset the unfavorable enthalpic aspects of the mixing of the three cations on one site, and yields an overall stability that is more favorable than either the substituted 1:2 or completely disordered perovskite alternatives.

While the X-ray studies and structure refinements provide direct support for the validity of the crystal chemical model of the 1:1 structure, they also give additional information on the size of the cation-ordered domains, which was previously shown to be important for optimizing the dielectric response of this system.[9] By monitoring the changes in the width of the ordering peaks in X-ray patterns collected during their synthesis, the size of the ordered domains in the 1:1 phases was found to increase to a final ''steady-state'' value. However, the size of the domains after final ''equilibration'' also showed a systematic increase with increasing *x*. For example, for $x = 0.04$ the domains were ~30 Å while they were calculated to be ~420 Å for $x = 0.25$. It is unclear whether these changes simply reflect small differences in the heat treatments or if they arise from some type of systematic change in the stability of the anti-phase domain boundaries (APBs) with composition. In either case it is clear that it is difficult to eliminate the APBs from the 1:1 random layer phases and, in contrast to the behavior of 1:2 ordered pure BZT, they are prevalent even after extended thermal treatment. It was suggested previously that these differences may be attributable to the lowering of the energies of the APBs through the presence of the random cation distributions on the β′ sites.[9]

Finally, we return to the correlations between the loss propertites and cation order in the BZT–BZ system. As noted previously, Tamura *et al*. had observed abrupt changes in the variation of *Q* with composition at substitution levels of ~4 and 25 mol% BZ.[2] Although the conditions of the sample preparation and processing in this study were slightly different from those used by Tamura *et al.*, it does seem to be significant that the changes in *Q* occur at almost exactly the same compositions that delineate the different types of cation order. While the highest *Q*'s are found in the region of stability of 1:2 ordering, albeit with some assistance from the Zr in stabilizing the domain boundaries, the 1:1 compositions also exhibit high *Q*. It is only when a transformation to a completely disordered perovskite has occurred that the *Q* values rapidly deteriorate.

Acknowledgments: We thank P. Woodward, J. B. Parise, Q. Zhu, D. Cox, W. Dmowski, and T. Egami for assistance in the structure refinement and synchrotron data collection.

References

[1]S. Kawashima, M. Nishida, I. Ueda, and H. Ouchi, ''$Ba(Zn_{1/3}Ta_{2/3})O_3$ Ceramics with Low Dielectric Loss at Microwave Frequencies,'' *J. Am. Ceram. Soc.*, **66**, 421–23 (1983).

[2]H. Tamura, T. Konoike, Y. Sakabe, and K. Wakino, ''Improved High-*Q* Dielectric Resonator with Complex Perovskite Structure,'' *J. Am. Ceram. Soc.*, **67**, C-59–C-61 (1984).

[3]S. B. Desu and H. M. O'Bryan, ''Microwave Loss Quality of $BaZn_{1/3}Ta_{2/3}O_3$ Ceramics,'' *J. Am. Ceram. Soc.*, **68**, 546–51 (1985).

[4]T. Negas, G. Yeager, S. Bell, and R. Amren, ''Chemistry and Properties of Temperature Compensated Microwave Dielectrics''; pp. 21–38 in *Chemistry of Electronic Ceramic Materials*, NIST SP 804. Edited by P. K. Davies and R. S. Roth. National Institute of Standards and Technology, Washington, DC, 1990.

[5]P. K. Davies, ''Influence of Structural Defects on the Dielectric Properties of Ceramic Microwave Resonators''; pp. 137–52 in Ceramic Transactions, Vol. 53, *Materials and Processes for Wireless Communication.* Edited by T. Negas and H. Ling. American Ceramic Society, Westerville, OH, 1995.

[6]S. Kawashima, ''Influence of ZnO Evaporation on Microwave Dielectric Loss and Sinterability of $BaZn_{1/3}Ta_{2/3}O_3$ Ceramics,'' *Am. Ceram. Soc. Bull.*, **72**, 120–26 (1993).

[7]F. Galasso, *Perovskites and High-T_c Superconductors*; pp. 3–72. Gordon and Breach, New York, 1990.

[8]A. J. Jacobson, B. M. Collins, and B. E. F. Fender, ''A Powder Neutron and X-ray Diffraction Determination of the Structure of $Ba_3Ta_2ZnO_9$: An Investigation of Perovskite Phases in the System Ba–Ta–Zn–O and the Preparation of $Ba_2TaCdO_{5.5}$ and $Ba_2CeInO_{5.5}$,'' *Acta Crystallogr.*, **B32**, 1083–87 (1976).

[9]P. K. Davies, J. Tong, and T. Negas, ''Effect of Ordering-Induced Domain Boundaries on Low-Loss $BaZn_{1/3}Ta_{2/3}O_3$–$BaZrO_3$ Pervoskite Microwave Dielectrics, *J. Am. Ceram. Soc.*, **80** [7] 1727–40 (1997).

[10]P. Woodward, R.-D. Hoffmann, and A. W. Sleight, ''Order–Disorder in $A_2M^{3+}M^{5+}O_6$ Perovskites,'' *J. Mater. Res.*, **9**, 2118–24 (1994).

[11]F. Izumi, ''Rietveld Analysis Programs RIETAN and PREMOS and Special Applications''; Ch. 13 in *The Rietveld Method.* Edited by R. A. Young. Oxford University Press, Oxford, U.K., 1993.

[12]A. C. Larson and R. B. Von Dreele, Report No. LA-UR-86-748, Los Alamos National Laboratory, Los Alamos, NM, 1987.

[13]G. K. Williamson and W. H. Hall, ''X-ray Line Broadening from Filed Aluminum and Wolfram,'' *Acta Metall.*, **1**, 22 (1953).

[14]S. A. Howard and K. D. Preston, ''Profile Fitting of Powder Diffraction Patterns''; Ch. 8 in *Modern Powder Diffraction.* Edited by D. Bish and J. Post. Mineralogical Society of America, Washington, DC, 1989.

[15]C. A. Randall and A. S. Bhalla, ''Nanostructural–Property Relations in Complex Lead Perovskites,'' *Jpn. J. Appl. Phys.*, **29**, 327–33 (1990).

[16]M. P. Harmer, J. Chen, P. Peng, H. M. Chan, and D. M. Smyth, ''Control of Microchemical Ordering in Relaxor Ferroelectrics and Related Compounds,'' *Ferroelectrics*, **97**, 263–74 (1989).

[17]J. Chen, H. Chan, and M. P. Harmer, ''Ordering Structure and Dielectric Properties of Undoped and La/Na-doped $Pb(Mg_{1/3}Nb_{2/3})O_3$,'' *J. Am. Ceram. Soc.*, **72**, 593–98 (1989).

[18]E. J. Fresia, L. Katz, and R. Ward, ''Cation substitution in Perovskite-like Phases,'' *J. Am. Chem. Soc.*, **81**, 4783–85 (1959).

[19]A. W. Sleight, J. M. Longo, and R. Ward, ''Compounds of Osmium and Rhenium with the Ordered Perovskite Structure,'' *Inorg. Chem.*, **1**, 245–50 (1995).

[20]G. Blasse, ''New Compounds with Perovskite-like Structures,'' *J. Inorg. Nucl. Chem.*, **27**, 993–1003 (1965).

[21]L. Padel, P. Poix, and A. Michel, ''Preparation and Crystallographic Studies of the System $Ba_2(UMg)O_6$–$Ba_2(U_{2/3}Fe_{4/3})O_6$,'' *Rev. Chim. Mineral.*, **9**, 337–50 (1972).

[22]A. D. Hilton, D. J. Barber, D. A. Randall, and T. R. Shrout, ''On Short Range Ordering in the Perovskite Lead Magnesium Niobate,'' *J. Mater. Sci.*, **25**, 3461–66 (1990).

[23]L. Chai, M. A. Akbas, P, K. Davies, and J. B. Parise, ''Cation Ordering Transformations in $Ba(Mg_{1/3}Ta_{2/3})O_3$–$BaZrO_3$ Perovskite Solid Solutions,'' *Mater. Res. Bull.*, **32** [9] 1261–69 (1997).

[24]K. Park, L. Salamanca-Riba, M. Wuttig, and D. Viehland, ''Ordering in Lead Magnesium Niobate Solid Solutions,'' *J. Mater. Sci.*, **29**, 1284–89 (1994).

[25]D. Viehland, N. Kim, Z. Xu, and D. A. Payne, ''Structural Studies of Ordering in the $(Pb_{1-x}Ba_x)(MG_{1/3}Nb_{2/3})O_3$ Crystalline Solution Series,'' *J. Am. Ceram. Soc.*, **78**, 2481–89 (1995).

[26]L.-J. Jin and T. B. Wu, ''Ordering Behavior of Lead Magnesium Niobate Ceramics with A-Site Substitution,'' *J. Am. Ceram. Soc.*, **73**, 1253–56 (1990).

[27]I. D. Brown, ''The Bond-Valence Method: An Empirical Approach to Chemical Structure and Bonding''; pp. 1–30 in *Structure and Bonding in Crystals*, Vol. 2. Edited by M. O'Keeffe and A. Navrotsky. Academic Press, New York, 1981.

[28]N. E. Brese and M. O'Keeffe, ''Bond Valence Parameters for Solids,'' *Acta Crystallogr*, **B47**, 192–97 (1991). □